

See discussions, stats, and author profiles for this publication at: <https://www.researchgate.net/publication/51247236>

Absolute Quantification of Intracellular Glycogen Content in Human Embryonic Stem Cells with Raman Microspectroscopy

ARTICLE *in* ANALYTICAL CHEMISTRY · JUNE 2011

Impact Factor: 5.64 · DOI: 10.1021/ac201581e · Source: PubMed

CITATIONS

25

READS

100

7 AUTHORS, INCLUDING:



Stanislav O Konorov

University of British Columbia - Vancouver

155 PUBLICATIONS **1,671** CITATIONS

SEE PROFILE



Chad G Atkins

University of British Columbia - Vancouver

8 PUBLICATIONS **95** CITATIONS

SEE PROFILE

Absolute Quantification of Intracellular Glycogen Content in Human Embryonic Stem Cells with Raman Microspectroscopy

Stanislav O. Konorov,^{†,‡} H. Georg Schulze,[†] Chad G. Atkins,^{†,‡} James M. Piret,^{†,§} Samuel A. Aparicio,^{||} Robin F. B. Turner,^{*,†,‡,⊥} and Michael W. Blades^{*,‡}

[†]Michael Smith Laboratories, The University of British Columbia, 2185 East Mall, Vancouver, British Columbia, Canada, V6T 1Z4

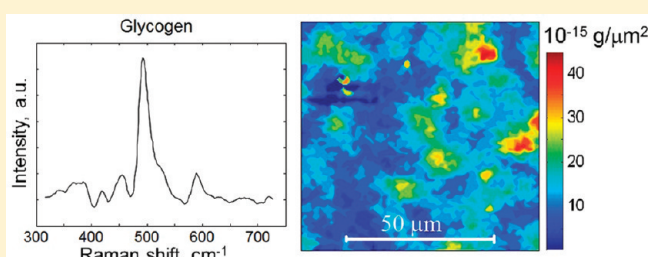
[‡]Department of Chemistry, The University of British Columbia, 2036 Main Mall, Vancouver, British Columbia, Canada, V6T 1Z1

[§]Department of Chemical and Biological Engineering, The University of British Columbia, 2360 East Mall, Vancouver, British Columbia, Canada, V6T 1Z3

^{||}Department of Pathology and Laboratory Medicine, The University of British Columbia, BC Cancer Research Centre, 675 West 10th Avenue, Vancouver, British Columbia, Canada, V5Z 1L3

[⊥]Department of Electrical and Computer Engineering, The University of British Columbia, 2332 Main Mall, Vancouver, British Columbia, Canada, V6T 1Z4

ABSTRACT: We present a method to perform absolute quantification of glycogen in human embryonic stem cells (hESCs) in situ based on the use of Raman microspectroscopy. The proposed quantification method was validated by comparison to a commonly used commercial glycogen assay kit. With Raman microspectroscopy, we could obtain the glycogen content of hESCs faster and apparently more accurately than with the kit. In addition, glycogen distributions across a colony could be obtained. Raman spectroscopy can provide reliable estimates of the in situ glycogen content in hESCs, and this approach should also be extensible to their other biochemical constituents as well as to other cell types.



Recently, it has been shown that infrared and Raman spectroscopy can be utilized to detect changes in cellular chemical composition.^{1–6} Raman spectroscopies constitute a family of coherent and noncoherent vibrational techniques that are suitable for use in aqueous media and hence with biological samples, and the power and utility of using molecular vibrations as a label-free, nondestructive contrast mechanism for bioimaging is well-established.⁶ Peaks in the Raman spectra can be attributed to particular cellular components, or combinations of them, and hence Raman spectroscopy can be a very powerful tool for determining the relative concentrations of biochemical components inside cells.^{7–9} In principle, Raman spectroscopy should also be useful for the *absolute* determination of biomaterial amount or concentration inside cells although this has yet to be definitively demonstrated.

Adding an internal standard at a known concentration to an investigated sample, assuming that the distribution of this internal standard is homogeneous within the volume of the sample,¹⁰ is a well-known method in analytical spectroscopy to determine absolute concentrations in an investigated sample. However, it is virtually impossible to introduce a noninvasive, homogeneously distributed, internal standard inside live cells. Here, we propose an alternative method for the absolute quantification of glycogen inside human embryonic stem cells (hESCs) that is relatively straightforward to implement.

Pluripotency, a capability of embryonic stem cells (ESCs)^{12–14} and induced pluripotent stem cells (iPSCs), is the ability to

differentiate into any adult cell type.^{15,16} For hESCs, pluripotency offers enormous therapeutic promise and hence has provoked intense research interest. However, to take full advantage of this potential, methods need to be developed to reliably induce and analytically validate that cells leave the pluripotent state and that sufficient cells of the desired phenotype and purity are obtained.¹⁷ This has motivated an increasing number of spectroscopic investigations of ESCs with a variety of specific analytical objectives. Previously glycogen was identified as the major contributor to the spectral variations in hESCs maintained under normal conditions.¹⁸ Intracellular glycogen content is a relevant analyte that would be useful to be able to determine quantitatively in different parts of the hESC colony.

MATERIALS AND METHODS

General Method. It is important to measure the absolute amounts or absolute densities of biochemical components of interest inside cells.^{18–24} Significant spatial glycogen variations¹⁸ occur within hESC colonies.

The proposed method requires a linear Raman signal dependence on the weight of the analyte per surface unit (surface density) in the

Received: April 7, 2011

Accepted: June 24, 2011

Published: June 24, 2011

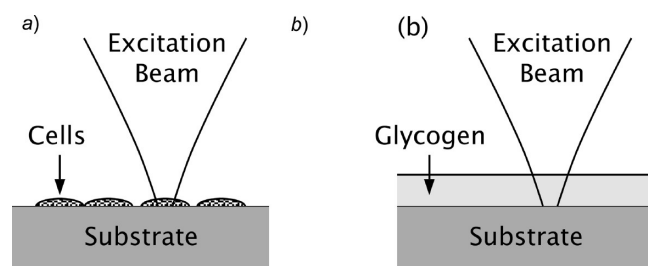


Figure 1. Schematic diagram of a cell to be investigated (a) and a layer of neat glycogen on top of the substrate for calibration (b). The microscope confocal parameter should be greater than the cell thickness.

investigated sample. This condition is necessary in order to use a surface density calibration curve. There are two common sources that could cause a deviation from linearity. One possibility is that sample absorption of either the pump laser radiation or Raman signal could reduce the signal, causing a deviation from linear dependence. Another is that different Raman signal collection efficiencies occur at different depths within the sample. For the method proposed here it is important to keep the cell thickness smaller than the laser beam confocal parameter (Figure 1a). This requirement can usually be achieved in the case of a monolayer of cells and a relatively large depth of focus (the objective lens should be $\times 50$ or less). We also assume that cells are transparent (i.e., have negligible absorption), a condition usually satisfied by monolayers of cells. CA1 hESC colonies typically grow as monolayers until confluence when colonies overgrow and should be subcultured. These monolayers are characterized by low absorption, a low refraction index contrast, as well as a thickness generally less than $10\ \mu\text{m}$. A $50\times$ objective in the Raman system used for this study satisfies both approximation criteria for a $10\ \mu\text{m}$ cell layer.

The first step of the procedure is to calibrate the Raman system to convert from the arbitrary readout counts of the detector to absolute surface density. Thus, it is necessary to find an appropriate calibration coefficient k for the type of substrate that is used for cell culturing and subsequent Raman spectral measurements. To do this, a carefully determined amount of neat glycogen should be distributed on top of the substrate. This glycogen should also satisfy the same criteria as measurements with cells (confocal parameter should be bigger than glycogen layer thickness and the glycogen layer should be transparent) (Figure 1b). However, in neither case is it necessary for the glycogen distribution to be homogeneous for Raman spectral acquisition if a sufficiently small scan step can be used, i.e., if the scan step is generally smaller than the glycogen nonhomogeneities.

We define the following calibration parameters relevant for a given scanned sample area: S , total scanned area (μm^2); m , total amount of material (g); N , total number of scanned points; M , total cumulative analyte signal strength (sum of counts from N points); r , averaged material density across area S ($\text{g}/\mu\text{m}^2$); k , the calibration coefficient ($\text{g}/\mu\text{m}^2/\text{count}$, glycogen density per Raman detector count).

The averaged material density can be expressed as

$$r = m/S = kM/N \quad (1)$$

Thus, k is given by

$$k = [m/S][N/M] \quad (2)$$

Cell Culturing. The CA1 hESC line was graciously provided by Dr. Andras Nagy (Mount Sinai Hospital Toronto, ON, Canada)

and maintained in Matrigel-coated (BD Biosciences, Mississauga, ON, Canada) culture dishes (Sarstedt, Montreal, QC, Canada) with mTeSR1 medium (STEMCELL Technologies, Vancouver, Canada). After adapting the CA1 hESC line for dispersed cell passing, cells were dissociated from their dishes using TrypLE (Invitrogen, Burlington, ON, Canada) according to the manufacturer's protocol. Cells were then plated on glass-encapsulated, Matrigel-coated mirrors and thereafter maintained with daily medium changes until used for spectroscopy. The mirrored substrates were used in order to improve the Raman signal intensities as previously described.¹¹ Each mirror consisted of gold thin-film on $12.7\ \text{mm}$ diameter, $6\ \text{mm}$ thick, glass discs with a $100\ \text{nm}$ encapsulating layer of noncytotoxic glass (ThorLabs Inc., Newton, NJ). The Matrigel coating was prepared by adding Matrigel diluted $1/30$ in DMEM/F12 (Invitrogen) followed by a $1\ \text{h}$ incubation at room temperature. Cell colonies were fixed with methanol prior to Raman measurements to preserve cellular composition and cellular structure.

hESC Staining. For detecting glycogen and indicating its approximate spatial distribution in hESC colonies, cultures on mirrors were stained with the magenta-colored periodic acid–Schiff (PAS) stain. Cells were fixed in neat methanol at $-30\ ^\circ\text{C}$ for $30\ \text{min}$. They were then rinsed three times with deionized water and incubated in 0.5% periodic acid for $5\ \text{min}$. Finally, the samples were washed three times with deionized water and subjected to Schiff stain for $2\text{--}3\ \text{min}$.

Glycogen Assay. PAS staining is a good and simple way to visualize glycogen distributions across hESC colonies. But this method is qualitative rather than quantitative. It is not possible to extract quantitative data from it due to nonhomogeneous glycogen staining from cell to cell as well as the presence of nonspecific background.

Instead, absolute glycogen quantification is routinely performed with glycogen assay kits based on glucoamylase that hydrolyzes the glycogen to glucose. The glucose is specifically oxidized to produce a product that reacts with an OxiRed probe to generate color ($\lambda_{\text{max}} = 570\ \text{nm}$) and fluorescence (Ex $535/\text{Em } 587$). The assay can detect glycogen over a range from 4×10^{-4} to $2\ \text{mg}/\text{mL}$. We used Biovision's glycogen assay kit (lot no. K646-100) to quantify intracellular glycogen in hESC.

However, even this method has drawbacks. It is not possible to do in situ; thus, the spatial distribution of glycogen across hESC colonies cannot be assessed. It requires sample sizes of at least several thousand cells, and it is destructive; moreover, it cannot yield close to real-time results. Overall, a complete analysis takes multiple hours and a range of tedious steps, including douncing to lyse the cells and multiple transfer events. In addition, the method requires a preliminary glucose removal step (before glucoamylase digestion of glycogen) to remove non-glycogen-bound glucose. It is difficult or virtually impossible to remove glucose completely, and this process varies dramatically from sample to sample. Another challenge comes from the fact that glycogen can be degraded very rapidly in some tissues after death (within a minute); therefore, special care, such as freezing samples immediately and keeping cold while working, must be taken to minimize glycogen loss when preparing cell samples. Furthermore, the kit is limited by the quality of the included reagents, all of which have a defined shelf life. The manufacturer's suggestion is that these reagents are viable within a 2 month window, but the quality of the assay may degrade noticeably thereafter. Thus, there are numerous unavoidable, as well as potentially undesirable, sources of error.

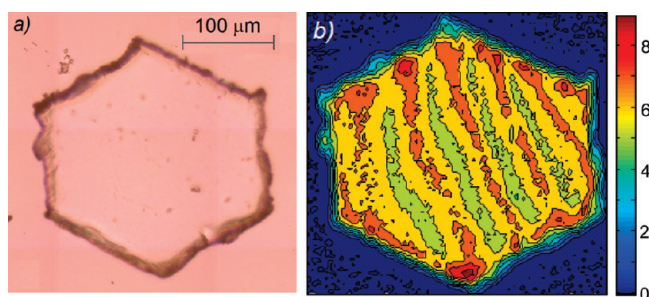


Figure 2. (a) Bright-field image of a polystyrene microcarrier. (b) Raman image at 1000 cm^{-1} of the same microcarrier.

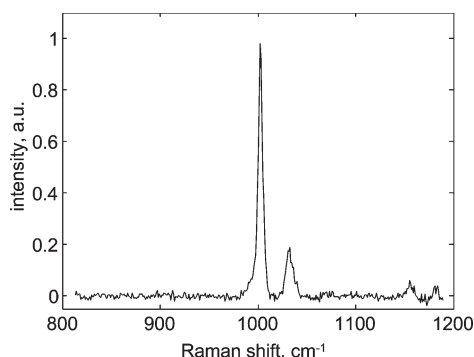


Figure 3. Raman spectrum of the polystyrene microcarrier.

Raman Measurements. Raman spectra were obtained with a Raman microscope system (InVia, Renishaw, Gloucestershire, U.K.) equipped with 785 nm and 80 mW excitation laser.

Polystyrene microcarriers (2D microhex, Nalge Nunc International, Denmark) and microspheres (Sigma-Aldrich) were used for method verification. The regular hexagonal microcarriers were well-characterized with a side length of $125\text{ }\mu\text{m}$ and a thickness of $25\text{ }\mu\text{m}$. Microspheres were $10\text{ }\mu\text{m}$ in diameter. We used a water-immersion $40\times$ objective lens to obtain Raman images from both samples in water to reduce the polystyrene/water refractive index contrast. Raman spectra were collected in the spectral range from 800 to 1200 cm^{-1} .

Neat bovine hepatic D-glycogen (Sigma-Aldrich, St. Louis, MO) was used to perform a Raman system calibration before measuring glycogen in cells. Glycogen Raman spectra were collected in the spectral range from 300 to 700 cm^{-1} . For neat glycogen the exposure time and objective used were 5 s and $\times 20$, respectively, and for cells they were 20 s and $\times 50$, respectively. Raman spectra were also obtained with both objectives from the same area of neat glycogen to adjust the signal intensity for the differential objective collection efficiencies.

RESULTS AND DISCUSSION

Calibration Coefficient Determination. A microcarrier (Figure 2a) was used to determine the calibration coefficient k by measuring the intensity of Raman scattering across the microcarrier (Figure 2b) based on the 1000 cm^{-1} polystyrene band (Figure 3) with a $\times 40$ objective and a $2.6\text{ }\mu\text{m}$ step.

One microcarrier contains $m = 1.4 \times 10^{-6}\text{ g}$ of polystyrene that can be calculated from the polystyrene microcarrier dimensions and its density. For this microcarrier the scanned area S was

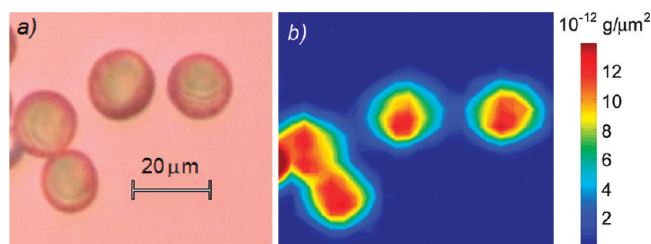


Figure 4. (a) Bright-field image of polystyrene spheres. (b) Raman image at 1000 cm^{-1} of polystyrene spheres.

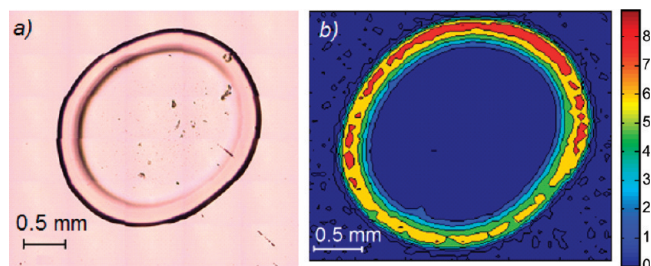


Figure 5. (a) Bright-field image of the evaporated glycogen droplet on top of the gold mirror. (b) Raman image at 485 cm^{-1} of the same glycogen droplet.

$7.4 \times 10^4\text{ }\mu\text{m}^2$, the number of points N was 10 920, and the cumulative signal strength M was 4.5×10^7 counts. Substituting these values into eq 1 gave, $k = 4.6 \times 10^{-15}\text{ g}/\mu\text{m}^2/\text{count}$

Calibration Coefficient Verification. Polystyrene spheres (Figure 4a) were used as an independent means of calibration coefficient verification. The Raman image of the polystyrene spheres (Figure 4b) was obtained by multiplying the polystyrene Raman line near 1000 cm^{-1} with the value of k obtained above ($4.6 \times 10^{-15}\text{ g}/\mu\text{m}^2/\text{count}$). Therefore, the image of the spheres is rendered in units of absolute density ($\text{g}/\mu\text{m}^2$). The maximum number density in these images ($\sim 13 \times 10^{-12}\text{ g}/\mu\text{m}^2$) occurs where the maximum sphere dimension is probed. Thus, the maximum number density ($\sim 13 \times 10^{-12}\text{ g}/\mu\text{m}^2$) divided by the known polystyrene density ($1.05\text{ g}/\text{cm}^3 = 1.05 \times 10^{-12}\text{ g}/\mu\text{m}^3$) should give the sample thickness ($\sim 12.4\text{ }\mu\text{m}$). This number is close to the mean diameter of the spheres ($\sim 15\text{ }\mu\text{m}$) seen in bright-field image (Figure 4a).

Glycogen Quantification Inside hESC. Next, we applied the method developed above to quantification of glycogen in hESCs. First, we determined the calibration coefficient k for neat bovine glycogen and then used this value to quantify glycogen in hESCs. The results were then compared to glycogen quantification from hESCs obtained with the glycogen assay kit.

Glycogen (45.1 mg) was dissolved in distilled water (3.2 mL), and $5\text{ }\mu\text{L}$ of the resulting solution, containing $70.5\text{ }\mu\text{g}$ of glycogen, was placed on the same type of gold mirror as used for Raman spectroscopy of hESCs and allowed to dry. The dry glycogen formed a smooth surface with an area of about 4 mm^2 (Figure 5a). Glycogen is distributed mainly on the edges of the droplet due to surface tension forces. Its Raman image (Figure 5b) was then obtained from the glycogen Raman marker line at 485 cm^{-1} (Figure 6) due to glycogen skeletal deformation.²⁵

The calibration coefficient was then calculated following the same procedure described above. The evaporated droplet shown in Figure 5 contains $m = 70 \times 10^{-6}\text{ g}$ of dry glycogen that was

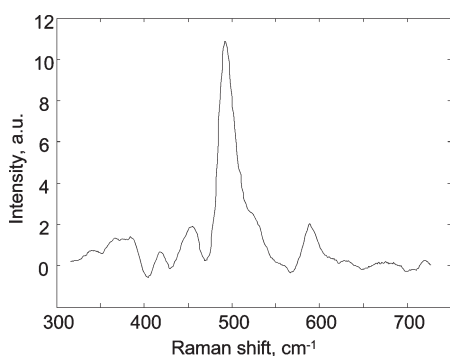


Figure 6. Glycogen Raman marker band at 485 cm^{-1} .

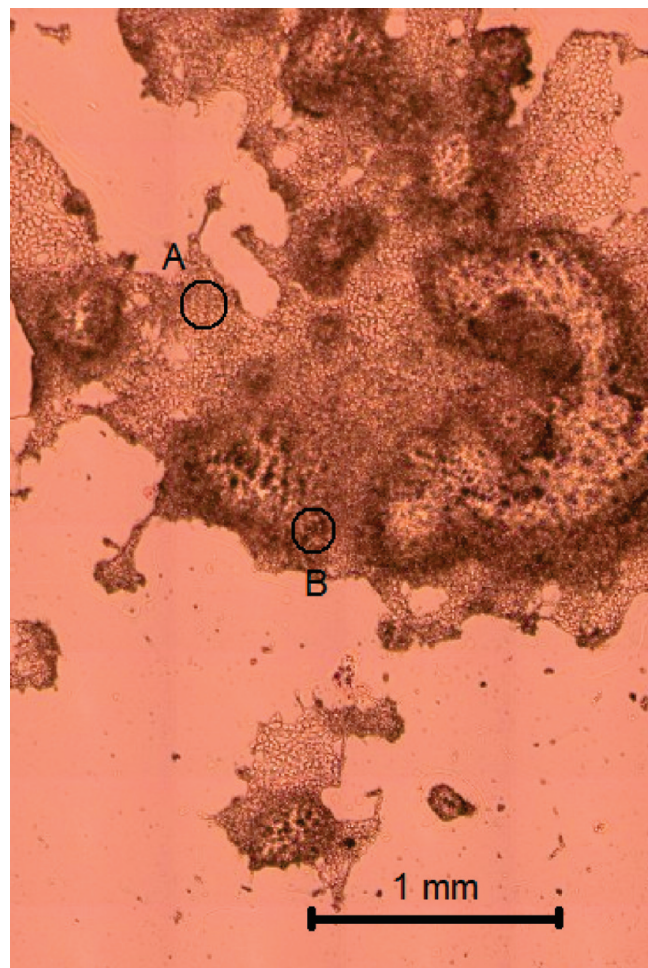


Figure 7. Bright-field image of the PAS-stained cells on top of the gold mirror. Dark areas correspond to higher glycogen concentration. Raman data were obtained, before PAS staining, from two areas with low (A) and high (B) glycogen concentration.

measured directly based on measured glycogen mass dissolved in water, the dilution, and solution volume used for calibration. For this glycogen the scanned area S was $7.67 \times 10^6\text{ }\mu\text{m}^2$, the number of points N was 3180, and the cumulative signal strength M was 6.6×10^6 counts. Substituting these values into eq 1 gave, $4.4 \times 10^{-15}\text{ g}/\mu\text{m}^2/\text{count}$. A correction was made to account for the different objective and the different exposure time used for the

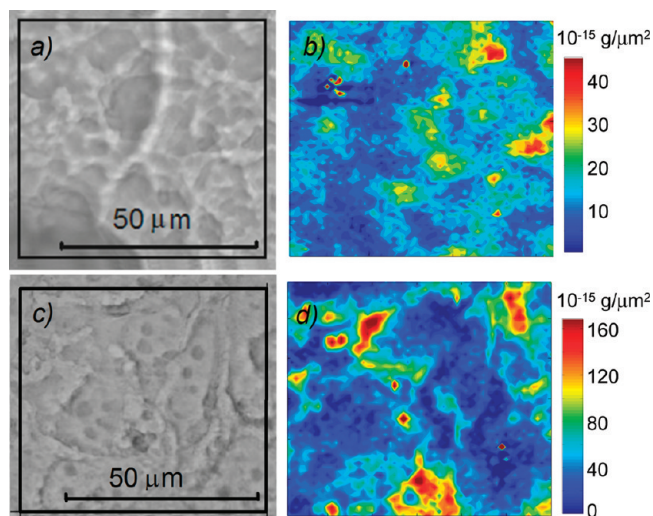


Figure 8. (a) Bright-field image of the PAS-stained cells with low glycogen concentration. (b) Raman image in the same area as plotted on panel a obtained based on intensity of the glycogen Raman line at 485 cm^{-1} multiplied by the calibration coefficient. (c) Bright-field image of the PAS-stained cells with high glycogen concentration. (d) Raman image in the same area as plotted on panel c obtained based on intensity of the glycogen Raman line at 485 cm^{-1} multiplied by the calibration coefficient.

glycogen calibration measurements ($\times 20$, 5 s) compared to measurements on methanol-fixed cells ($\times 50$, 20 s). After correction, the calibration coefficient obtained for hESCs was $k = 2.2 \times 10^{-16}\text{ g}/\mu\text{m}^2/\text{count}$.

On the basis of previous experience,¹⁸ we selected two locations in the colony where we expected to find low (location A, Figure 7) and high (location B, Figure 7) glycogen levels. Raman images of glycogen distributions were obtained at both locations before PAS was applied. The average hESC diameter is about $10\text{--}15\text{ }\mu\text{m}$; thus, the average cell area, when viewed two-dimensionally, is about $120\text{ }\mu\text{m}^2$.

The calibration coefficient was then applied to the Raman image based on the glycogen marker band near 485 cm^{-1} to create an image of absolute number or surface density of glycogen. The Raman signal obtained from the same area shows good reproducibility. The average signal intensity ($\sim 90 \times 10^{-15}\text{ g}/\mu\text{m}^2$) around the bright spot in the bottom of the picture (Figure 8d), multiplied by the average cell area of $120\text{ }\mu\text{m}^2$, then gave a glycogen content of about 10 pg per cell in the area selected for high glycogen content. For the low glycogen content area, a value of about 3 pg per cell was obtained. These values compared very favorably to the duplicate values of 5.5 and 2.9 in one experiment and 15 pg per cell in another experiment obtained with the glycogen assay kit. The mean \pm SEM from the kit triplicates was 7.8 ± 3.7 pg per cell, within the range established by the Raman measurements. The reader is reminded that the kit assay was performed on large numbers of cells and that the assay values approximated averages. Thus, in order to assess the comparative performance of the method, we also determined an average glycogen content, but from a second hESC sample. In this sample, 2916 evenly spaced spectra obtained from a 65 by $54\text{ }\mu\text{m}^2$ area gave an average glycogen content of about 5 pg per cell.

In contrast to the glycogen assay kit and previous quantitative Raman work where analyses were performed on cell suspensions

and on cell pellets,²³ thus providing average values, the present Raman approach provided not only quantitative information but also a more quantitative view of actual glycogen distributions within the colony. Such glycogen variations within colonies of hESCs are in agreement with previously published results.¹⁸

The proposed method can be extended to live cells as well, but it will require calibration measurements of solvated/hydrated glycogen to mimic the state of glycogen inside living cells covered by an aqueous medium layer. Glycogen is highly soluble in water, and some thin coating on top of the neat glycogen might be sufficient to avoid this effect.

CONCLUSION

We have developed a technique to perform absolute glycogen quantification in hESCs in situ. The Raman signal from an investigated sample should be linearly proportional to the amount of analyte in the sample in order to apply this method. In practice, it assumes two conditions must be satisfied: first, the sample should be well within the collection volume such that the Raman signal could be collected from a total interrogation volume with a height that exceeds the height of the investigated sample. Second, the cell sample, as well as the neat calibration sample, should be transparent and with a low elastic scattering efficiency. These are usually valid for a cellular monolayer. We validated our technique against a widely used glycogen assay kit. A very favorable comparison (well within uncertainty of the glycogen quantification kit) was obtained between the Raman method and a glycogen quantification assay with both methods yielding similar quantitative results. Because we have previously used Raman microspectroscopy to investigate live hESCs under similar conditions without apparent adverse consequences to their pluripotency,^{17,18} we fully expect this technique to be effective in live cells as well. Moreover, in principle, this technique should also be extensible to other cell types, such as hepatic, cardiac muscle, nerve, and brewer's yeast (*S. cerevisiae*) cells, where glycogen metabolism is of great interest.^{26–29} This approach should also be extensible to the quantification of other cellular components of interest provided that the above conditions are satisfied. Being able to quantify major cellular components in live cells, in situ and in real time, would be of considerable benefit to hESC research.

AUTHOR INFORMATION

Corresponding Author

*E-mail: turner@msl.ubc.ca (R.F.B.T.); blades@chem.ubc.ca (M.W.B.). Fax: 604-822-2114 (R.F.B.T.); 604-822-2847 (M.W.B.).

ACKNOWLEDGMENT

We are grateful to Chris Sherwood for his invaluable help with the cell culturing and glycogen assay. Instrumentation and infrastructure were provided by the UBC Laboratory for Advanced Spectroscopy and Imaging Research (LASIR) and Laboratory for Molecular Biophysics (LMB). Funding was provided by the Natural Sciences and Engineering Research Council (NSERC), the Canadian Institutes of Health Research (CIHR), the Michael Smith Foundation for Health Research (MSFHR), the Canada Foundation for Innovation (CFI) and the British Columbia Knowledge Development Fund (BCKDF). The first two authors contributed equally to this work.

REFERENCES

- (1) Ami, D.; Neri, T.; Natalello, A.; Mereghetti, P.; Doglia, S. M.; Zanon, M.; Zuccotti, M.; Garagna, S.; Redi, C. A. *Biochim. Biophys. Acta* **2008**, 1783, 98–106.
- (2) Chan, J. W.; Lieu, D. K.; Huser, T.; Li, R. A. *Cell Res.* **2008**, 18, S130.
- (3) Chan, J. W.; Taylor, D. S.; Lane, S. M.; Zwerdling, T.; Tuscano, J.; Huser, T. *Anal. Chem.* **2008**, 80, 2180–2187.
- (4) Lau, A. Y.; Lee, L. P.; Chan, J. W. *Lab Chip* **2008**, 8, 1116–1120.
- (5) Matthäus, C.; Chernenko, T.; Newmark, J. A.; Warner, C. M.; Diem, M. *Biophys. J.* **2007**, 93, 668–673.
- (6) Nottingher, I.; Bisson, I.; Bishop, A. E.; Randle, W. L.; Polak, J. M. P.; Hench, L. L. *Anal. Chem.* **2004**, 76, 3185–3193.
- (7) Gaus, K.; Rösch, P.; Petry, R.; Peschke, K.-D.; Ronneberger, O.; Burkhardt, H.; Baumann, K.; Popp, J. *Biopolymers* **2006**, 82, 286–290.
- (8) Kim, B. S.; Lee, C. C. I.; Christensen, J. E.; Huser, T. R.; Chan, J. W.; Tarantal, A. F. *Stem Cells Dev.* **2008**, 17, 185–198.
- (9) Koljenovic, S.; Bakker Schut, T. C.; Wolhuis, R.; de Jong, B.; Santos, L.; Caspers, P. J.; Kros, J. M.; Puppels, G. J. *J. Biomed. Opt.* **2005**, 10, 031116.
- (10) Konorov, S. O.; Schulze, H. G.; Addison, C. J.; Haynes, C. A.; Blades, M. W.; Turner, R. F. B. *J. Raman Spectrosc.* **2009**, 40, 1162–1171.
- (11) Konorov, S. O.; Schulze, H. G.; Caron, N. J.; Piret, J. M.; Blades, M. W.; Turner, R. F. B. *J. Raman Spectrosc.* **2011**, 42, 576–579.
- (12) Thomson, J. A.; Itskovitz-Eldor, J.; Shapiro, S. S.; Waknitz, M. A.; Swiergiel, J. J.; Marshall, V. S.; Jones, J. M. *Science* **1998**, 282, 1145–1147.
- (13) Trounson, A. *Endocr. Rev.* **2006**, 27, 208–219.
- (14) Odorico, J. S.; Kaufman, D. S.; Thomson, J. A. *Stem Cells* **2001**, 19, 193–204.
- (15) Vats, A.; Bielby, R. C.; Tolley, N. S.; Nerem, R.; Polak, J. M. *Lancet* **2005**, 366, 592–602.
- (16) Chen, H.-F.; Kuo, H.-C.; Chien, C.-L.; Shun, C.-T.; Yao, Y.-L.; Ip, P.-L.; Chuang, C.-Y.; Wang, C.-C.; Yang, Y.-S.; Ho, H.-N. *Hum. Reprod.* **2007**, 22, 567–577.
- (17) Schulze, H. G.; Konorov, S. O.; Caron, N. J.; Piret, J. M.; Blades, M. W.; Turner, R. F. B. *Anal. Chem.* **2010**, 82, 5020–5027.
- (18) Konorov, S. O.; Schulze, H. G.; Piret, J. M.; Turner, R. F. B.; Blades, M. W. *J. Raman Spectrosc.* **2011**, 42, 1135.
- (19) Schmid, A.; Kortmann, H.; Dittrich, P. S.; Blank, L. M. *Curr. Opin. Biotechnol.* **2010**, 21, 12–20.
- (20) Bechtel, K. L.; Shih, W.-C.; Feld, M. S. *Opt. Express* **2008**, 16, 12737.
- (21) Pilling, J.; Garside, H.; Ainscow, E. *Mol. Cell. Biochem.* **2010**, 341, 73–78.
- (22) Shamsaie, A.; Heim, J.; Yanik, A. A.; Irudayaraj, J. *Chem. Phys. Lett.* **2008**, 461, 131–135.
- (23) Borland, L. M.; Kottegoda, S.; Phillips, K. S.; Allbritton, N. L. *Annu. Rev. Anal. Chem.* **2008**, 1, 191–227.
- (24) Mourant, J. R.; Dominguez, J.; Carpenter, S.; Short, K. W.; Powers, T. M.; Michalczyk, R.; Kunapareddy, N.; Guerra, A.; Freyer, J. P. *J. Biomed. Opt.* **2006**, 11, 064024.
- (25) Lyng, F. M.; Faoláin, E. Ó.; Conroy, J.; Meade, A. D.; Knief, P.; Duffy, B.; Hunter, M. B.; Byrne, J. M.; Kelehan, P.; Byrne, H. J. *Exp. Mol. Pathol.* **2007**, 82, 121–129.
- (26) Pilling, J.; Garside, H.; Ainscow, E. *Mol. Cell. Biochem.* **2010**, 341, 73–78.
- (27) Pederson, B. A.; Chen, H.; Schroeder, J. M.; Shou, W.; DePaoli-Roach, A. A.; Roach, P. J. *Mol. Cell. Biol.* **2004**, 24, 7179–7187.
- (28) de Almeida Souza, A.; Seixas da Silva, G. S.; Veleza, B. S.; Santoro, A. B. M.; Montero-Lomeli, M. *Neurosci. Lett.* **2010**, 482, 128–132.
- (29) Parrou, J. L.; François, J. *Anal. Biochem.* **1997**, 248, 186–188.